ETH zürich

Master thesis report

Estimation of the infiltration rate from an artificial lake in Guantao County, China

Author:

Alexandre Mérillat

Professor:

Prof. em. Dr. Wolfgang Kinzelbach

Supervisor:

Gianni Pedrazzini

Acknowledgements

I would like to thank everybody who contributed in this project by sharing their knowledge of the topic and the study site or by their practical help.

First and foremost, my gratitude goes to Ge Xiaotong for collecting our data, running the experiment and taking care of our material for almost two months after we left Guantao.

I would like to thank Prof. em. Dr. Wolfgang Kinzelbach and his team for their support and assistance. I am thankful to Dr. Wang Lu for her help in the contact with our Chinese partner and for her translations, and to Dr. Li Ning for her helping me understanding the theoretical background of my study and providing me useful data. I wish to express my gratitude to Gianni Pedrazzini for his committed supervision and to Prof. Em. Dr. Wolfgang Kinzelbach himself for providing me the opportunity to work in this interesting project.

Finally, as this work represent the term of my engineering studies, I would like to thank my parents and family for their support during the last seven years. I am also extremely grateful to my fiancé Sarah for her support and endless patience during this demanding project.

Contents

Table of figures

Abstract

The present MSc thesis evaluates the infiltration capacity of an artificial lake in the North China Plain, China. High precision pressure sensors were used to measure the water level of the lake and the evaporation. A water balance was calculated, and the infiltration could be estimated.

The mean infiltration rate from the lake over the study period was 0.037 m/day. An estimation of the infiltration rate prior to the experiment gave a mean infiltration rate of 0.13 m/day for that period, yet this estimation remains arguable. The difference between these infiltration rates is due to progressive clogging of the lake bed. The hydraulic conductivity of the clogging layer is in the vicinity of 0.30 - 0.55 m/day.

The total infiltrated volume is 106,303 m^3 over the infiltration event. Infiltration was practiced twice between spring 2015 and spring 2016 with an estimated total infiltrated volume of 200,000 m^3. This annually infiltrated volume covers 4% of the average annual water deficit in Guantao during the period 2001 - 2012.

The long-term sustainability of artificial infiltration in Guantao is discussed. Concerned are raised about a reduction of infiltration rate due to a progressive raise of the water table around the lake.

Possible reasons for clogging and mitigation measures are discussed. The most probable reason for clogging is deposition of fine particles, yet this should be further investigated before any conclusion about clogging can be drawn. A summary of possible further research and investigation is given as an outlook.

1 Introduction

The increase of water use over the 20th century, linked with a technological leap in pumping technology as well as cheap and abundant energy led to over-pumping of aquifer in many arid and semi-arid regions of the globe (Konikow & Kendy, 2005). Climate change could make the precipitation patterns more irregular, forcing populations to rely even more on depleting groundwater (Taylor, 2012). The resulting effects, such as depletion of surface water by an increased infiltration rate, salinization of soils and soil subsidence, led to a worldwide awareness of the need for sustainable groundwater management.

My MSc thesis takes place in a general groundwater management project in the North China plain, China: "Rehabilitation and management strategy for over-pumped aquifers under a changing climate". According to the project proposal to the Swiss Development Agency (IfU & Hydrosolutions, 2014), the project aims to achieve sustainable groundwater management practices through modern monitoring and modelling. First, two test sites were chosen, one in the Heihe river basin (Luotuocheng, a desert area) and one in the North China plain (Guantao, Hebei province, a semi-arid climate). Both present specific and distinct topography, climate, and water use. The project will create new technologies and knowledge that will be useful for other arid and semi-arid regions (Project proposal, 2014).

There are three main approaches to reducing groundwater stress: reallocation, reduced use, and supply augmentation (Molle, 2003). Reallocation and reduced use are always possible, but sometimes at a high societal, economic or ecological cost. Therefore, supply augmentation techniques (artificial recharge) have been developed for a range of situations (Bouwer, 2002).

Artificial recharge is practiced worldwide and has proven itself especially useful in annually varying climates, where a wet season is followed by a dry season. The water surplus from the wet season can be stored for the next dry season. Although artificial recharge techniques have been extensively studied, the high number of variables influencing the infiltration makes it difficult to predict the efficiency of the process, so that an on-site assessment is still the only reliable estimate of the efficiency of a project (Bouwer, 2002).

Multiple artificial recharge lakes have been built in Guantao County. The current master thesis aims to assess the efficiency of those lakes, as such work has not been done before. First, an experimental setup was built on-site to measure the change in water level and other relevant data for a simple seepage model. The infiltration rate and other aspects of the groundwater behaviour were estimated from those data by water balance and Darcy's law. Finally, the relevance of these data for the current project is discussed and complementary and alternative solutions are discussed.

2 Method

2.1 Theoretical background

My work is based on two common tools of hydrology and groundwater modelling: water balance (derived from the principle of continuity) and Darcy's law.

The simplest form of water balance is expressed as

$$\frac{dV(t)}{dt} = \sum Q_{in}(t) - \sum Q_{out}(t) \qquad (1)$$

Where dV/dt is the change of volume per time unit [m^3/day], $\sum Q_{in}$ is the sum of all inflows [m^3/day], and $\sum Q_{out}$ is the sum of all outflows [m^3/day]. Those quantities can be expressed either as either as [$volume_{water}$/time], like above, or as [$height_{water}$/time], provided that the geometry of the water container is known.

For a simple lake, where there is neither inflows nor outflows of water, equation (1) simplifies to

$$\frac{dh_{lake}(t)}{dt} = 0 \ - (E(t) + I(t)) \qquad (2)$$

Where dh_{lake}/dt is the change of water level in the lake per time unit [m/day], E is the evaporation rate [m/day] and I the infiltration rate [m/day]. All terms in equations (1) and (2) are time-dependent.

Darcy's law expresses the flow of a fluid through a porous medium between two points. The flow is equal to the conductivity of the medium multiplied by the gradient between the two points. In the case of a flow from a surface water body to an aquifer, the formulation of Darcy's law depends on whether the water body is connected to the aquifer through saturated soil or not. If it is connected, Darcy's law is expressed as:

$$V_i = K\frac{dh}{dL} \qquad (3)$$

Where V_i is the Darcy velocity (or Darcy flux, in [$m^3/(m^2 \cdot day)$]). V_i is the flow of water through a unit area per time unit. V_i multiplied by the cross sectional area of the medium gives the total flux of water through the medium (Q, in [m^3/day]). K is the hydraulic conductivity [in m/day] in the direction of the flux and dh/dL is the gradient [m_y/m_x]. If the water body isn't connected to the aquifer, Darcy's law is expressed as:

$$V_i = K\frac{H_w + L_f \ - h_{we}}{L_f} \qquad (4)$$

Where H_w is the height of water above the ground [m], L_f, the depth of the wetting front from the ground [m], and h_{we} [m] is the capillary suction. Figure 1 shows schematic diagrams of connected and unconnected aquifers.

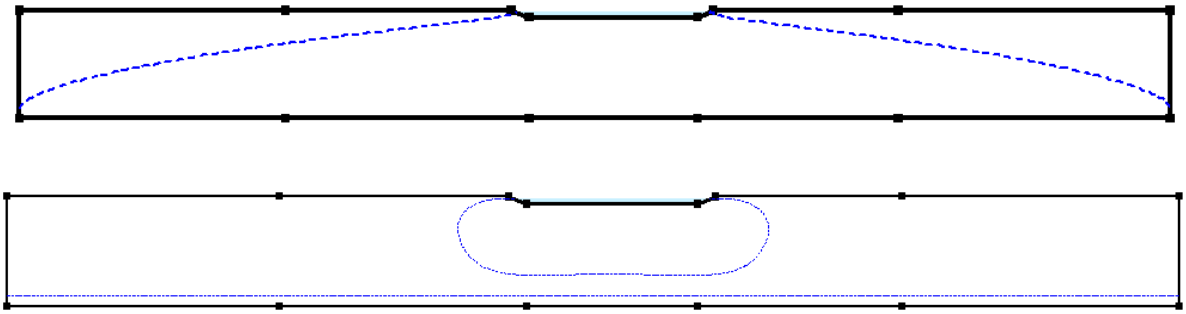

Figure 1: Schematic diagram of infiltration from a surface water body. Top: connected to the aquifer. Bottom: unconnected.

2.2 The test site

The groundwater management project has two pilot sites: Heihe river basin and Guantao County. Our test site is at the south of Guantao County. The site is located in a farming area and contains a canal, two artificial lakes and approximately thirty irrigation wells. The canal brings water from the Weiyun River to the area. The two lakes were built recently and serve mostly for artificial recharge, but could also be used for short-term storage of excess water. The lakes are connected to the canal through weirs that can be closed. The irrigation wells are scattered over the fields, yet we chose to limit our measurements to a line of boreholes perpendicular to the lake shore and one extra borehole very close to the lake shore (see 3.1.5). Figure 2 shows an aerial view of the test site.

The test site is mostly flat with an average elevation of 42 m a.s.l. Several villages surround the area and Guantao Township is located north-west of the test site (Figure 3).

Figure 2: Aerial view of the test site. The aerial pictures are from 2011 and Lake 2 was in construction. The construction of Lake 1 has not started yet. BH denotes the boreholes we used for groundwater monitoring.

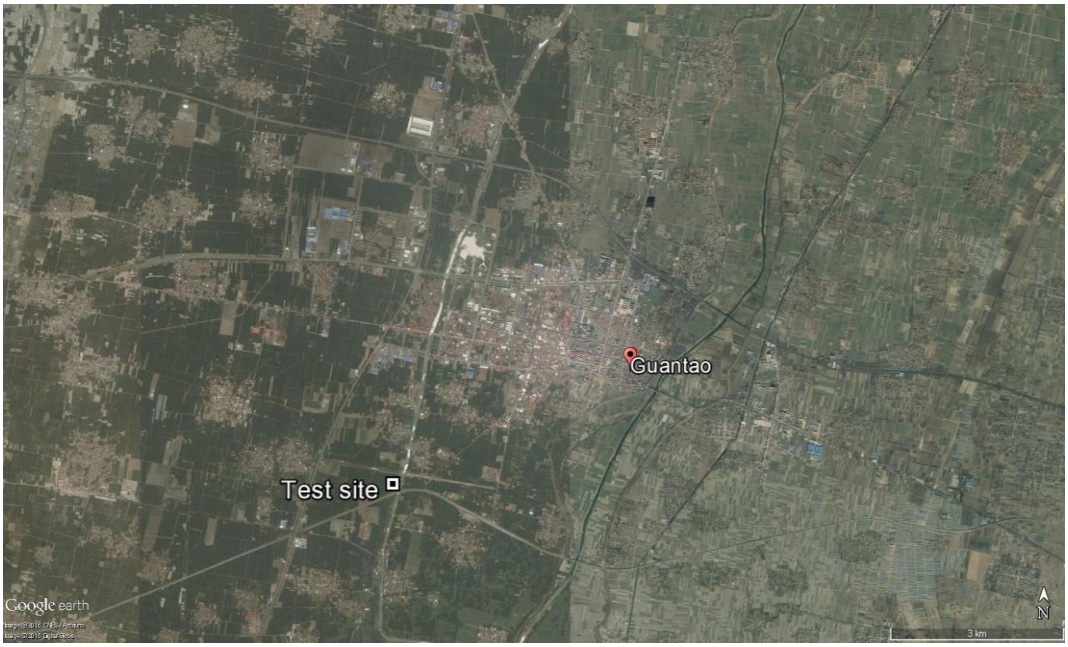

Figure 3: Aerial view of Guantao Township and position of our test site.

The only water inflow in the lakes are direct inflow from the canal and precipitation. Water exchange (in both directions) with the canal happens by gravity when the weir is open. The weir is located higher than the bottom of the lake and the river. Once the water level is too low in both water bodies, the direct connection is lost and the canal and lakes can only be connected through groundwater.

There was no connection through the weir during most of our measurement campaign, and the status of the connection through the aquifer is unclear. For two days, Lake 1 received water from the canal. The water exchange prior to our arrival remains unclear, as the water level was probably high enough for exchange to happen between Lake 1 and the canal during many days and we have no information about the status of the weir.

The possible outflows from the lakes are evaporation and infiltration. Besides those quantifiable inflows and outflows, water pumping in and from the lakes is the other possible source of change in water storage. This happened during our study sometimes, and the concerned periods were ignored in the analysis.

Figure 4: Pictures of the test site.
Left: Lake 1, right: the canal

2.3 Pressure sensor and logger

We used high precision pressure sensors with loggers to measure the water level. Each logger consists of two sensors and a memory. It is separated in two solid parts linked by a cable, each part containing one sensors which measures pressure and temperature. One sensor must be under water while the other must stay in the air. The loggers records the temperature and the pressure at both location. The difference between the two measured pressures gives water pressure at the location of the water sensor, from which the height of the water column is calculated. The measurement of real-time air pressure allows to correct the variation of air pressure over time, which would create inaccuracy in the water pressure estimation.

The loggers were set up to take one measurement of every variable every second and store the averages value every four minutes. Since the loggers have an internal memory of 2 MB, this allows the storage of 4 weeks of continuous measurement. Besides, the four minutes average filters most high-frequency disturbances, such as waves. Figure 5 shows the logger. The precision of the pressure sensor is discussed in appendix E.

Figure 5: The logger. The left sensor is submerged, the right sensor is placed above the water surface (contains the internal memory and the interface to read the data).

2.4 Evaporation pan

An evaporation pan was built to measure the evaporation component of the lake water balance. It consists of a round, waterproof pan made of stainless steel filled with water. Since the water can only evaporate, the observed level difference over time gives an approximation of the evaporation from water bodies in the area. The pan itself has a diameter on 80 cm and a height of 24 cm. The pan was put on the water, at the south of Lake 1.

Several features were included in the pan to reduce measurement errors. The pan was put on a stabilising structure made of two crossed wood slats with expanded polystyrene (EPS) floaters at their tips. The slats are 3 m long and the EPS floaters are rectangular cuboids of roughly 40x35x25 cm. This structure ensures a great stability to the pan and makes it unsinkable, as the mass density of the ensemble is lower than that of water. Although the pan lays on the structure, it is still in contact with the lake water, even when empty. This ensures that the water temperature, which is an important parameter for evaporation, stays the same in the pan as in the lake surface. Wave-breaker were built around the pan to avoid external input of water through

waves. They consist of a metal sheet square around the pan (30 cm minimal distance to the pan).

The water level was measured with a pressure sensor located in the middle of the pan, where the oscillation of water level due to waves is minimal. The sensor is protected by a metal tube. The pan was positioned in the middle of the lake to ensure similar weather conditions (solar irradiance, wind) as those prevailing for most of the water body. This position is also a protection against theft and vandalism, as most locals don't know how to swim. The pan is linked to the shore by a cable system and can be pulled to the shores and back to the lake. This system allows easy data reading and maintenance in the course of the experiment. An experienced operator needs less than five minutes to pull the pan from the measurement position to the shore. Figure 6 shows the pan on-site.

The pan was designed by Gianni Pedrazzini and Alexandre Mérillat, and built by Gianni Pedrazzini. The supporting structure for the pan was built on-site by Gianni Perdazzini, Alexandre Mérillat, Ge Xiaotong, and You Jin.

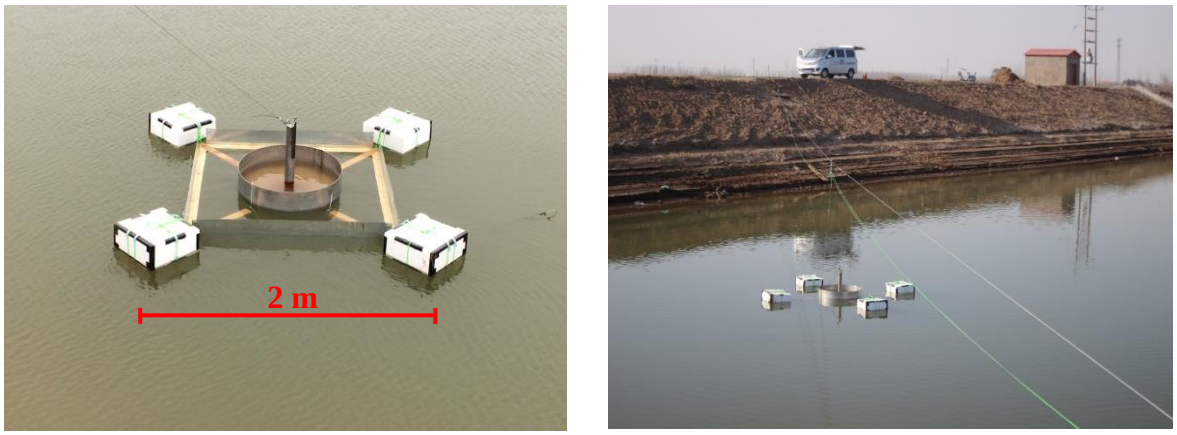

Figure 6: The evaporation pan on site.
Left: The evaporation pan. The change of water level in the pan is measured by a pressure logger in the central tube. The wooden structure with EPS floaters stabilises the pan and prevents sinking in case of a storm. The metal sheet protect the pan from water spilling in by wave.
Right: The cable system to connect the pan to the shores. The system allows to pull the pan to the shores and back to the lake easily and can be blocked to fix the pan in a given location.

2.5 Sensor structure

Since the sensor is made of flexible parts, it has to be put in a solid structure to immobilise it and protect it. The specification requirements for the structure were the following:

1. A solid structure that immobilise the sensor. Any movement of the sensor will add an error to the measurement. A fast movement can be detected visually on the data plot; slow movements might not, yet the error remains.

2. The structure should be movable by an operator within a reasonable time. As the sensor must always remain partly under water and partly in the air (2.3), this allows a response to an important change in water level.

3. The sensor must be easy to hide and must be protected against vandalism or various disturbances: animals, children playing, scavengers, etc.

The structure we built is shown in Figure 7 (left). Two sensor structures were used on site, one at the north of Lake 2, the other at the south of Lake 1.

The water level in the river was measured with a simple pressure and temperature sensor. Unlike the double sensors, it does not measure air pressure and temperature, and is entirely submerged. The sensor was connected to the shore with a cable and put inside a stabilising anchor. The anchor was put in the water. Figure 7 (right) shows the anchor for the river sensor.

The sensor structures were built on site by Gianni Pedrazzini, Alexandre Mérillat, Ge Xiaotong, and You Jin.

Figure 7: The sensor structure.
Left: the entire structure for lake sensors.
Right: the anchor for the river sensor.

2.6 Topographic survey

The elevation of the the marks for hand measurements at the two lakes and the canal, and of each borehole were measured with a dumpy level. Due to time constraints, the survey was conducted only in one direction, without loop. The level bias was measured and the results were corrected accordingly.

Since the absolute elevation of the area was not known with certainty, it was decided that all elevations would be expressed as relative elevation with regard to the elevation of the fix point for hand measurements at the river. The elevation of this point was set to 100 m to avoid negative elevations of some points. In this system, all points have a virtual elevation between 95 m and 105 m.

Besides, a drone flight was organised by our partner university in Handan. The result is an aerial photograph of the study site with some elevation measurements. Appendix A shows the photograph of the study site.

2.7 Other measurements

Small-scale measurements were done besides the one described above. Soil and water samples were taken, mostly to have a rough estimate of the water quality and the soil composition. The water depth in the boreholes was measured with a dip meter.

2.7.1 Double-ring infiltrometer tests

Double-ring infiltrometer tests were conducted at the shores of the canal and Lake 1 to estimate the vertical hydraulic conductivities of the shores. The infiltrometer was positioned at approximately 1 m from the water, so that the soil would be dry under it and be similar to the soil of the shore under water. The infiltration rate was measured in the inside ring with a pressure logger. The infiltration from the outside ring makes the flow from the inside ring vertical and allows the measurement of the vertical hydraulic conductivity.

The change in water level from the infiltrometer is much faster than the infiltration rate from the lake. This difference is due to the gradient in Darcy's law governing the flow. In the lake, the gradient at the shore is almost horizontal, whereas in the infiltrometer, this gradient is vertical, thus creating a much faster Darcy velocity. Figure 17 shows the double-ring infiltrometer and the water level over time in the inside ring.

Figure 8: double-ring infiltrometer test. Left: the infiltrometer setup seen from above, before the start of the experiment. Right: the infiltrometer working on-site.

2.8 Continuation of the experiment after our departure

The experiment was continued after we left by local student under their professor's supervision. The student went to the test site every second week, read data from the loggers and filled a sheet with their measurements and visual observations. Appendix B shows a filled data sheet, and appendix B shows the timeline of the experiment.

3 Results and discussion

3.1 Raw results

3.1.1 Water levels in the lakes and the canal

The following water level time series were obtained with the method described in appendix D. Figure 9 shows the water level in Lake 1, Lake 2 and in the canal. The long blanks in the time series are due to logger failures (programming mistakes by the operator). Short blanks are times of data reading and maintenance. Data are missing for Lake 2 after 17th April because the sensor was lost.

The Pearson product-moment correlation coefficient between hand measurements and sensor measurements are: 0.999 for Lake 1 (8 values), 0.994 for Lake 2 (5 values) and 0.971 for the canal (8 values). Those correlation coefficients are very high and show that the method used to correct the sensor time series (appendix D) gives excellent results. The water level change in Lake 1 is the fastest, followed by Lake 2 and the canal.

Figure 10 shows the water level over time in Lake 1 more in details. The water level change is comparatively fast at the beginning and then slows down. Reasons for this behaviour are discussed in 3.2.

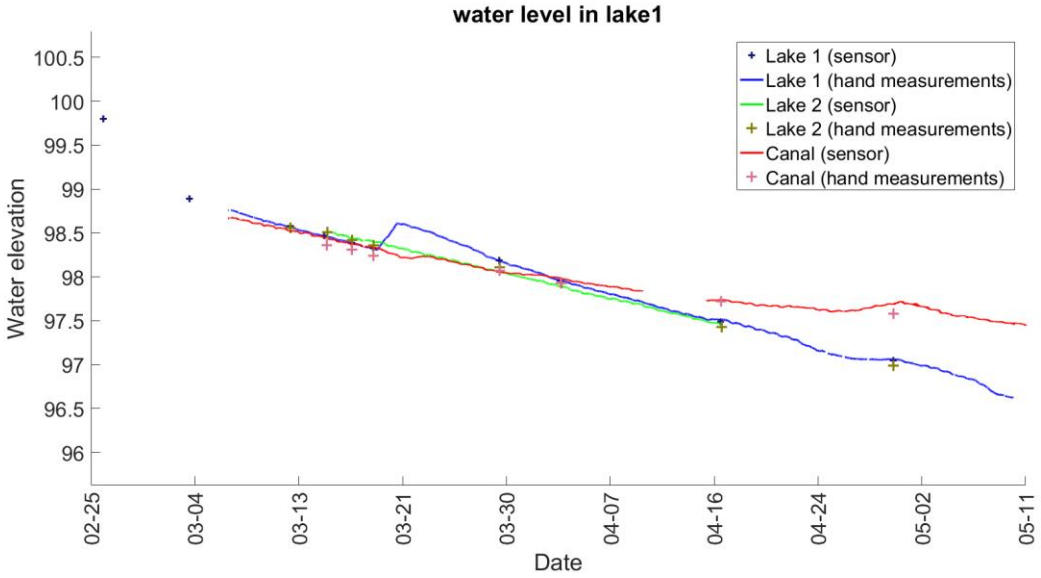

Figure 9: Water elevation over time in Lake 1, Lake 2 and in the canal.

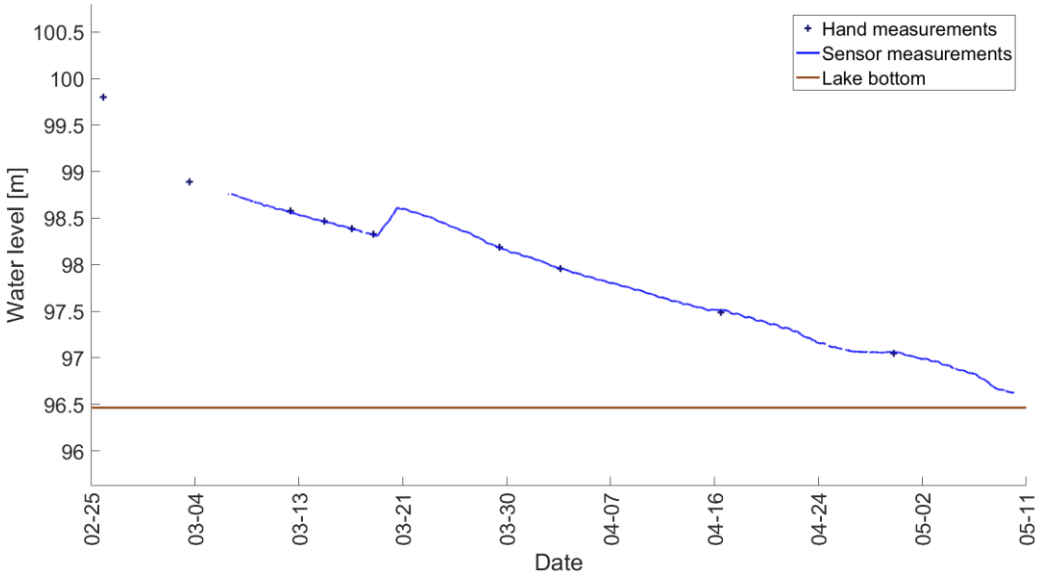

Figure 10: Water height in Lake 1 over time. The hand measurements before the start of the sensor time series are estimations of earlier water levels based on observation of dust traces on concrete structures and discussion with the local water authorities.

3.1.2 Evaporation rate

The evaporation rate was measured by the evaporation pan. The cumulative evaporation curve shown in Figure 11 was created with the procedure described in appendix D. The cumulative evaporation during the 52 days of measurements was 0.19 m (9th March – 30th April). A logger failure prevented the record of evaporation for the last two weeks of the experiment, so those values were estimated using the Linacre formula (Linacre, 1977). This formula calculates the daily evaporation from the geographic position (elevation and latitude), the mean daily temperature and the mean daily dew point. The calculated evaporation doesn't reproduce the measured values, yet the standard deviation between the two series remains small (1.8 mm/day) compared to the daily infiltration rate from the lake (37 mm/day, see 3.2). The definitive time series used in the water balance is a combination of the measured values filled with the calculated values when measured values are missing.

Figure 12 shows the computed and measured values. On average, the evaporation counts for 11.45% of the water balance during the measurement and simulation period. However, the general part of evaporation in the water balance for the whole infiltration is only 9.11%, because the infiltration rate prior to our measurement campaign was higher (3.5).

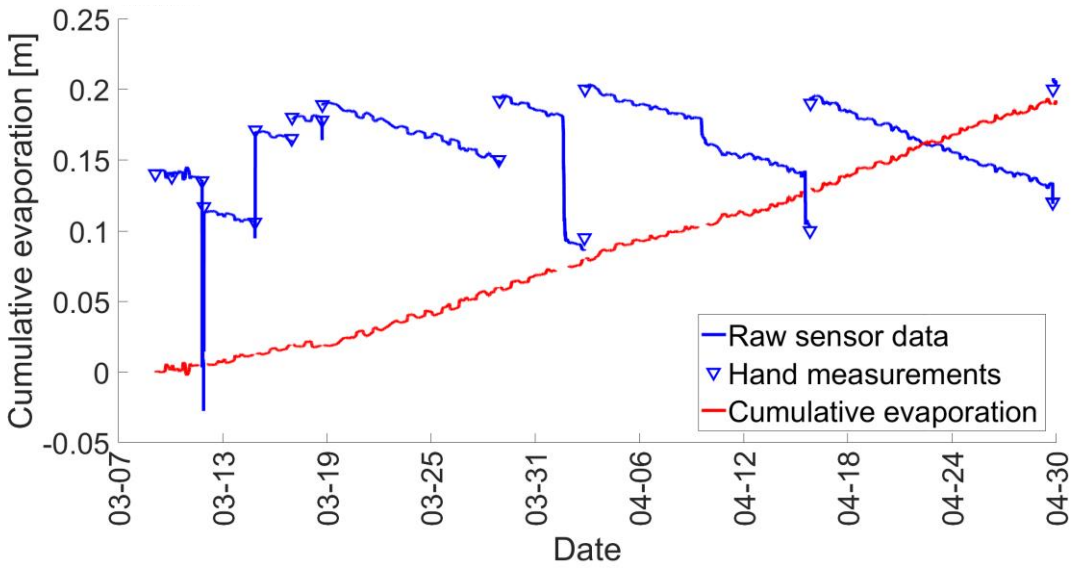

Figure 11: cumulative evaporation from the pan. The evaporation logger stopped working two weeks before the end of the experiment, hence the need to complete the time series with calculated evaporation.
The blue line are the raw water level measurements from the sensors. The blue triangles are the hand measurements. The jumps in the raw water level measurements are periodic refills of the pan. The water level was measured before and after refilling.
The red line is the cumulated evaporation.

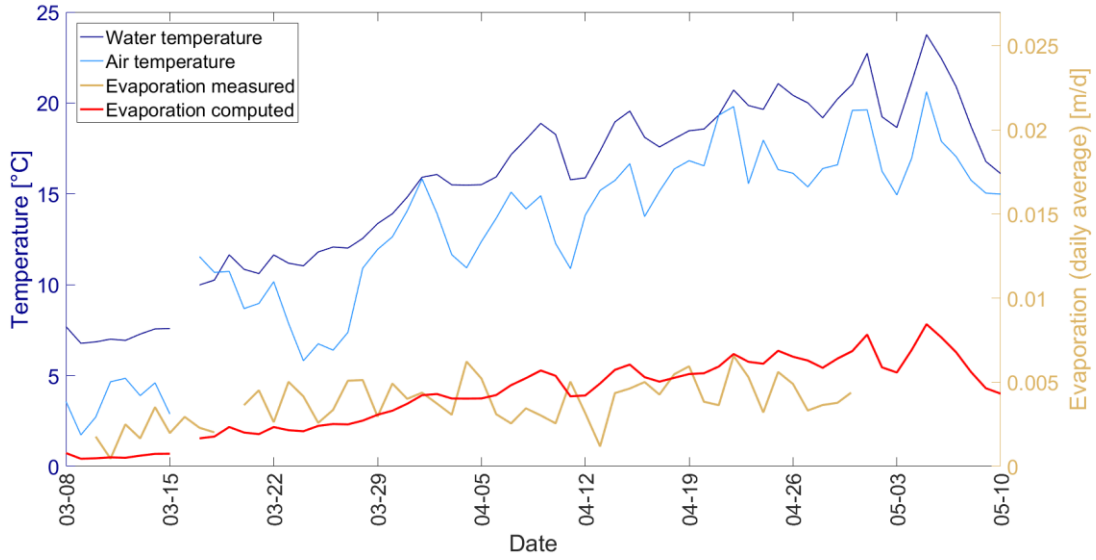

Figure 12: computed and measured evaporation. The computed evaporation doesn't reproduce the daily variation of evaporation, yet it is always within the same range as the measured evaporation (standard deviation = 1.8 mm).

3.1.3 Soil samples

Soil samples were taken on the shores of both lakes and of the river, and on a degraded portion of the southern lake shore, where ground collapsing had made the undisturbed soil layers visible. The samples were analysed visually. There are two main types of soil on the profile, one has a light brown to beige colour and the other has a darker brown colour. The light brown soil is coarser than the dark brown one. The light brown soil is probably a sandy loam, while the dark brown one is a silt loam or a clay loam.

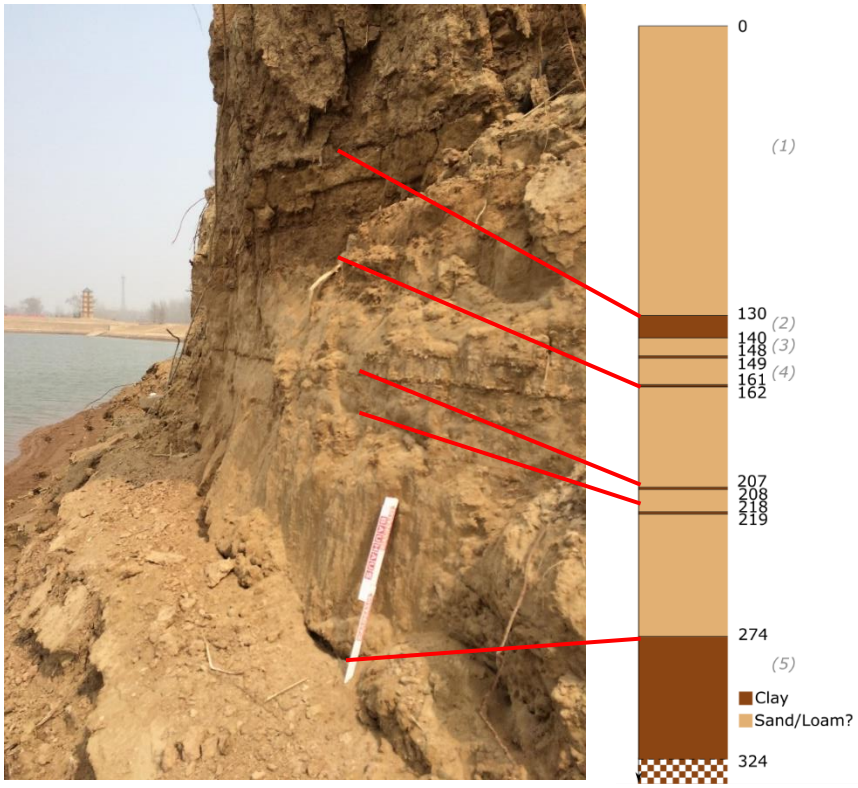

(a) (b)

Figure 13: Soil layers. (a) Site at which the samples were taken. The lake shore collapsed at this location and revealed an undisturbed soil
(b) Soil profile [cm under the ground level]. The number in grey parentheses represent the origin layer of soil samples.

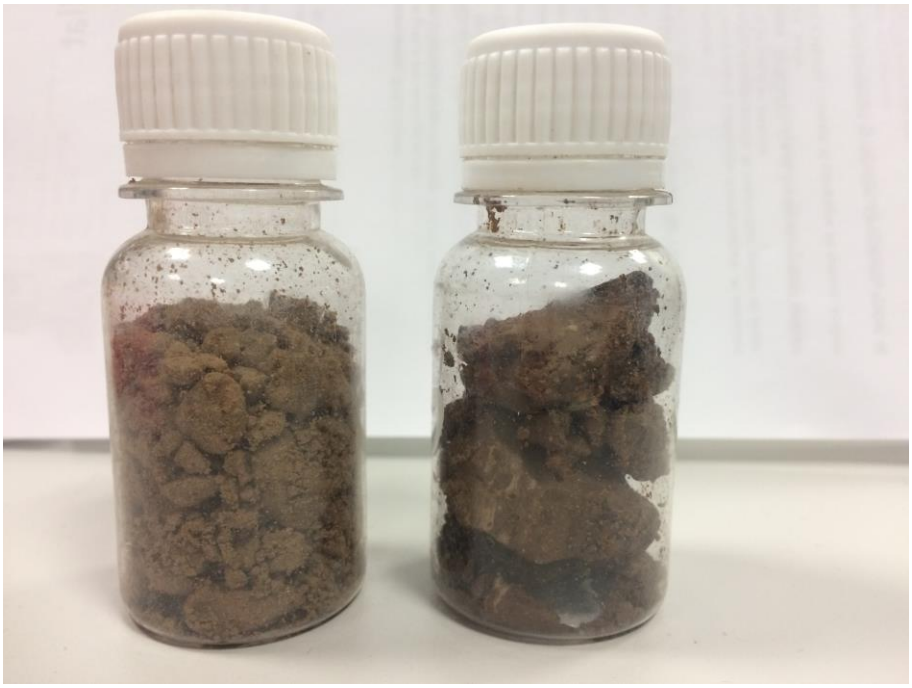

Figure 14: Soil samples. Left: presumably sandy loam, appears light brown in Figure 13. Right: presumably clay loam or silt loam, appears dark brown in Figure 13.

3.1.4 Water samples and water composition

Water samples from Lake 1 and from the canal were taken. The water in the canal was turbid and had a yellow colour. The water from the lake was less turbid. Figure 15 presents pictures of both samples.

Figure 15: Water samples from the canal (left) and from Lake 1 (right). The pictures were taken more than two month after sealing, when particles already flocculated. The turbidity is higher in the river than in the lake, as visible by the size and number of flocculated particles.

3.1.5 Water level in boreholes

We chose to measure the water level in seven boreholes along a perpendicular line to the lake shore and ignore the others, except one borehole very near to the lake. Compared to the measurement of water levels in randomly scattered boreholes, the water level in boreholes on a line gives a more reliable picture of the water level in the surroundings of the lake and needs little post-processing. Moreover, the line is parallel to the supposed direction of the water flux, so that the flow problem simplifies to a 1D-problem.

Boreholes 1 to 6 are located on an almost straight line at the west of the lake and perpendicular to the shore (Figure 2). Boreholes 7 and 8 are not on the line, but they were added to the profile under the assumption of a spatially uniform seepage from the lake. The water level in borehole 5 could not be read because the borehole was clogged. The shape of the water table suggests that the lake is connected to the aquifer. Figure 16 presents the profile.

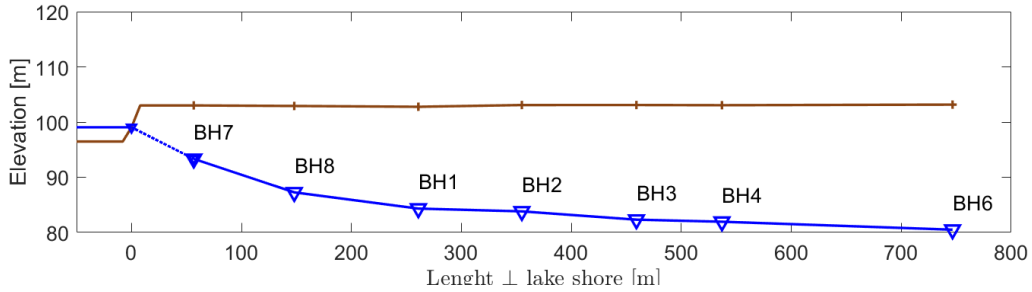

Figure 16: Water level in the boreholes on 10th March, before the start of pumping for irrigation. The connection between the lake and the groundwater table was assumed from the curve shape. The vertical scale is exaggerated for better visibility (scale 5:1 compared to the x-axis).

3.1.6 Double-ring infiltrometer tests

Double-ring infiltrometer tests were conducted at the shores of the canal and Lake 1. Figure 17 shows the water level over time in the inside ring for both sites.

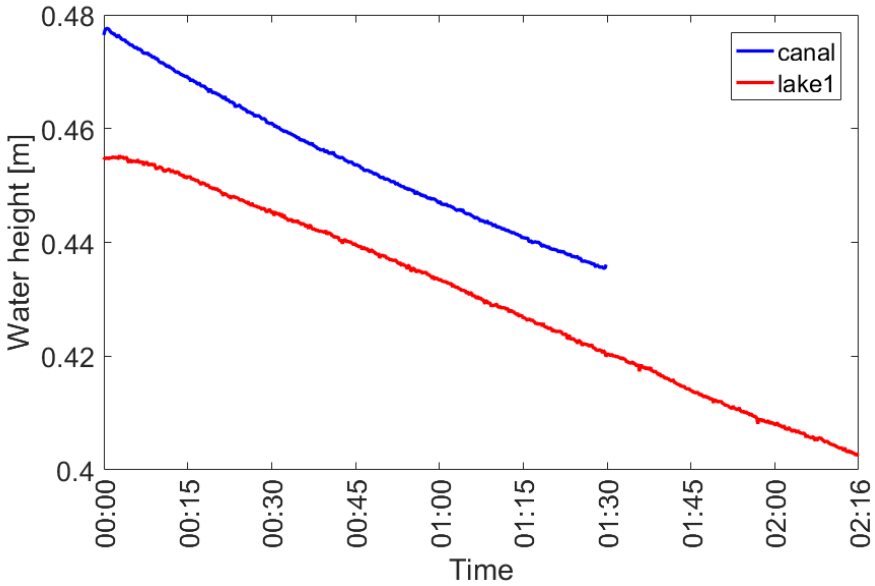

Figure 17: The water level in the inside ring over time. 00:00 is the start of the experiment.

3.2 Infiltration rate from Lake 1

The infiltration rate from Lake 1 was calculated as follows:

$$I_w = \frac{dh_{lake} - E_{net}}{\Delta t} \text{ [m/day]} \qquad (5)$$

Where E_{net} is the net evaporation [m] and dh_{lake} [m] the level difference of the lake during the period Δt. The water level measurements are very sensitive and the imprecision is high (3.7.4). For this reason, the infiltration rate was computed on a 3 days moving average of daily values. In some periods, the influence of other factors on the level difference of the lake was too high and the infiltration calculated from those level measurements is wrong. Therefore, those measurement were removed from the daily infiltration time series before applying the moving-average filter. Possible reasons for those measurements errors are discussed in 3.6. Figure 18 shows the change in infiltration rate over time, and Figure 19 shows the relation between the depth

and the infiltration rate. The average infiltration rate over the measurement period was 0.037 m/day with a 95% confidence interval of [0.025, 0.049].A trend is visible between the water depth and the infiltration rate: the infiltration rate increases positively with the water depth. However, this relationship is not straightforward and shows a significant noise, as various unmeasured factors influence it. Some factors are partially known, such as the influence of the Darcy gradient (2.1, 3.3.1), others are completely unknown, especially clogging. For those reasons, the trend in the relationship between water depth and infiltration rate is shown as a line. The real trend is probably not linear, yet the linear trends help to estimate the infiltration rate for a given depth.

The maximal water level can be read from the dust traces left on concrete structures (see Figure 10). At such an elevation, the lake water was most probably connected to the canal through the weir. Therefore, equation (2) does not apply to calculate the infiltration rate, unless the weir was closed right after filling or the water exchange with the canal is insignificant. This would be the case if the infiltration rate from the canal would be similar to the one from the lake and the water level would sink at the same rate in both water bodies.

Assuming that one of the two conditions above was met, the infiltration rate can be estimated to be roughly 0.13 m/day. This infiltration rate is much higher than the one during our measurement period. If our assumption is verified and the initial infiltration rate was higher than the one during our measurement period, it means that the infiltration rate was either driver by a steeper Darcy gradient or a higher hydraulic conductivity. We will see further that the hydraulic conductivity of the lake shores is unusually low for the region (3.3), indicating the probable presence of a clogging layer on the lake bed. A higher infiltration rate at the beginning of the infiltration period would mean that the clogging layer was formed during the infiltration event, probably by deposition of fine particles (3.6).

Whether clogging happened during the infiltration event which we monitored or not, the lake is clogged and will remain so, unless measures are taken to remove the clogging layer. If no maintenance is done, the infiltration behaviour of the lake will resemble the one shown by the linear interpolation in Figure 19 and never reach higher values again.

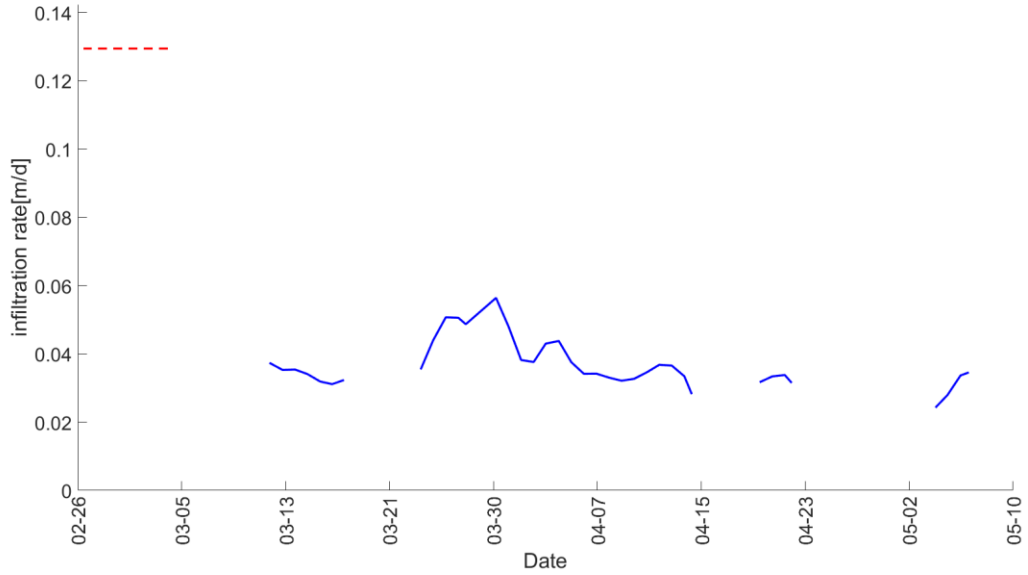

Figure 18: time series of daily infiltration. A 3-days moving average was applied to the time series. The high infiltration at the beginning of the time series, represented in a dotted line, is an average of the infiltration rate prior to our arrival on site.

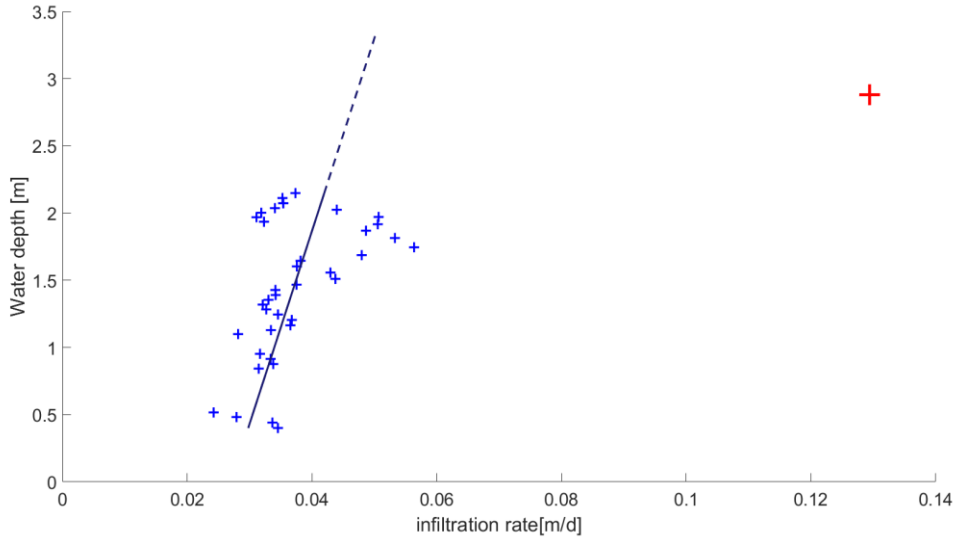

Figure 19: infiltration rate vs. water depth. Water depth is represented on the vertical axis for readability reasons. The dark blue line is a linear interpolation of the infiltration rate and the depth calculated from the sensor measurements. The dashed, dark blue line is an extrapolation of this relation for depth values prior to our experiment. The red point in the left of the plot is the mean infiltration and water depth prior to our arrival, estimated from dust marks on concrete structures.

3.3 Hydraulic conductivity

3.3.1 Vertical hydraulic conductivity

The vertical hydraulic conductivity was measured by Darcy's formula under the assumption of a connection between the lake and the aquifer (2.1). Under the Dupuit-Forchheimer assumption, the water infiltrating from the lake must flow through a cylindrical surface located between the lake shores and the bottom of the aquifer. I made the simplifying assumptions that the bottom of the aquifer is flat and that the Darcy gradient at the lake shore is uniform all around the lake. Under those assumptions, a Darcy velocity can be calculated from the infiltrated volume and the surface between the lake shore and the bottom of the aquifer.

$$V_i = \frac{dV/dt}{S_{lake-aqu}} = \frac{\frac{dh}{dt} \cdot A_{lake}}{P_{lake} \cdot H_{lake-aqu}} = 0.021 \text{ m/day} \qquad (6)$$

Where $S_{lake\text{-}aqu}$ is the horizontal surface between the lake shore and the bottom of the aquifer [m^2], dh/dt is the level difference of the lake on the day when the water level in boreholes was measured [m/day] (3.1.5), A_{lake} is the area of the lake [m^2], P_{lake} is its perimeter [m], and $H_{lake\text{-}aqu}$ is the height between the lake shore and the bottom of the aquifer [m]. The relevant gradient for the infiltration is the gradient of the water table at the interface lake-aquifer (the lake shore, since the lake is connected). Since it could not be measured directly, I approximated it by the gradient between the lake shore and borehole 7 (see Figure 2 and Figure 16). The aquifer thickness in the area is 79 m under the ground (Chinese Geological Bureau, 2015). The height of the lake water table from the aquifer bottom is therefore 74.6 m. This results in a hydraulic conductivity of

$$V_i = K\frac{dh}{dL} \rightarrow K_{vert} = V_i\left(\frac{dh}{dL}\right)^{-1} = 0.223 \text{ m/day}. \qquad (7)$$

The hydraulic conductivity calculated with this method is an order of magnitude smaller than the hydraulic conductivity in the area given by the Chinese geological bureau (3.3 m/day, 2015). As the infiltration from the lake is limited by the clogging layer, the hydraulic conductivity measured here is the one of the clogging layer, not the one of the aquifer in general.

3.3.2 Horizontal hydraulic conductivity

The horizontal hydraulic conductivity was measured by the double-ring infiltrometer test (3.1.6). Since the water in the infiltrometer is a priori not connected to the aquifer, equation (4) applies to calculate the hydraulic conductivity. The hydraulic conductivity measured is the one of the limiting layer, i.e. the clogging layer. After simplifications, the equation for K is (Bouwer, 2002):

$$K_{hor} = \frac{\Delta y}{\Delta t} \cdot \frac{\Delta y_{tot}/n_{eff}}{\bar{z} + \Delta y_{tot}/n_{eff} - h_{we}} \qquad (8)$$

Where Δy [m] is the change of water level in the infiltrometer during Δt [day], $\bar{z}$ [m] is the average water height in the infiltrometer during Δt, n_{eff} is the effective porosity [-], and h_{we} is the capillary suction at the wetting front [m]. $\Delta y_{tot}/n_{eff}$ represent the depth of the wetting front in equation (4). For a better estimation, $\Delta y/\Delta t$ was calculated over the last hour of the experiment, when the infiltration rate was stable.

Of those six parameters, only four (Δy, Δy_{tot}, Δt, and $\bar{z}$) were measured by the sensor. Assumptions must be made for the effective porosity and the capillary suction. Three assumptions of porosity and two assumptions of capillary suction were made based on observations made on-site. For the effective porosity, the assumptions were:

1. $\mathbf{n_{eff}}$ **= 0.15**. This porosity would be the one of a sandy loam, a likely soil type of the lake shore.

2. $\mathbf{n_{eff}}$ **= 0.10**. This is an intermediate porosity between the sandy loam and the clay loam.

3. $\mathbf{n_{eff}}$ **= 0.05**. This porosity would be the one of a clay loam.

The assumptions for the capillary suctions were:

1. $\mathbf{h_{we}}$ **= -0.25 m**. This is the capillary suction of a sandy loam (Bouwer, 2002).

2. $\mathbf{h_{we}}$ **= -0.35 m**. This is the capillary suction of a loam or a structured clay (Bouwer, 2002).

Table 1and Table 2 show the hydraulic conductivities resulting from the assumptions. The vertical hydraulic conductivities are within the same order of magnitude as the horizontal one, but they are always higher (at least 150% higher). This result is contrary to the usual behaviour of anisotropic soils. Part of it can be explained by the fact that the behaviour of the clogging layer is not anisotropic a priori, therefore the vertical and horizontal hydraulic conductivities could be similar. Another source of error is the infiltration of water at the cylinder-soil interface. If the cylinder creates a preferential leakage path through the clogging layer, the infiltration rate will be affected, and subsequently the hydraulic conductivity will be overestimated. Finally, different methods can lead to different hydraulic conductivities values measured at the same

site. Difference of up to one order of magnitude have been reported (Landon, Rus, & Harvey, 2001).

Table 1: Vertical hydraulic conductivity values for Lake 1 [m/day] resulting from different assumptions. Results from contradictory assumptions are not shown.

	n_{eff} = **0.15**	n_{eff} = **0.10**	n_{eff} = **0.05**
h_{we} = **-0.25 m**	0.38	0.43	-
h_{we} = **-0.35 m**	-	0.51	0.54

Table 2: Vertical hydraulic conductivity values for the canal [m/day] resulting from different assumptions. Results from contradictory assumptions are not shown.

	n_{eff} = **0.15**	n_{eff} = **0.10**	n_{eff} = **0.05**
h_{we} = **-0.25 m**	0.33	0.39	-
h_{we} = **-0.35 m**	-	0.47	0.52

3.4 Infiltration rate from the canal

A direct measurement of the infiltration rate from the canal with water balance is not possible. The canal is more than 30 km long, which is too long to have a complete control of all the inflows and outflows. The biggest inflow to the canal is at its beginning, from the Weiyun River, and we do not know it. Yet there is a way to estimate the infiltration rate: the vertical hydraulic conductivities measured with the double-ring infiltrometer at the canal and at the lake are very close, and they are close to the horizontal hydraulic conductivity calculated from the well cross-section. If the hydraulic gradient is the same at both locations, the true infiltration rate is very likely to be close to the infiltration rate of the lake (3.2).

3.5 Total infiltrated volume

The total infiltrated amount was calculated from the total infiltrated head and the shape of the lake. To simplify our calculations, we shall assume that the total infiltrated head is the product of the duration of the infiltration period and the mean infiltration rate. The mean infiltration head was calculated from the linear interpolation for water depths ranging between zero and the maximal observed water depths from the dust traces (3.33 m; see Figure 10 and Figure 19). The mean infiltration rate is 0.04 m/day, and the infiltration period was 74 days, which gives a total infiltrated head of 2.96 m.

The average surface of the lake during this period was calculated from the maximal surface of the lake (i.e. the surface of the excavation), the average slope read from the drone flight map, and the average water level during the infiltration. The resulting surface is S = 35,899 m^2.

The total infiltrated water is then:

$$V_{inf} = H_{tot} \cdot S = 106{,}303 \text{ m}^3 \quad (9)$$

We have previously discussed the possibility of a higher infiltration rate at the beginning of the infiltration period. The volume estimated above does not account for this eventuality, and is therefore a rather conservative estimation. Moreover, a lake without clogging layer could infiltrate a bigger volume during the same time span, or infiltrate the same amount quicker.

According to Mr Yao, our contact on site, the lake was filled twice last year. This yields a total infiltrated volume of nearly 200,000 m^3 in a year. The average storage change in Guantao between 2001 and 2012 was $-5 \cdot 10^6$ m^3/a (*Annual report*, 2016). This means that the infiltration from one lake could cover 4% of the water deficit in the county, or that 25 lakes could cover the entire yearly water deficit.

3.6 Clogging

Clogging most likely happens at Lake 1, with the formation of a clogging layer in the lake bed (3.3). However, the nature of this clogging remains unknown.

Figure 15 shows water samples from the canal and from Lake 1. There is a difference in turbidity between those two water bodies. The true reason for the turbidity is unknown, yet I retain two hypotheses: high organic carbon content or high fine particle content. In reality, both are probably true to some extent, yet I shall consider them separately. A high organic carbon content would lead to biochemical clogging of the soil by bacteria using the organic carbon, whereas a high fine particle content would lead to deposition of fine particles and subsequently clogging. In both cases, the difference in turbidity between the canal water and the lake water could indicate a clogging process in Lake 1.

Biological activity is not a plausible hypothesis at the time of the year when we did the experiment, because the temperature was low. Therefore, the main reason for clogging in is probably the deposition of fine particles.

The water in the canal was really turbid (Figure 4). The water in the lake was turbid during windy days, but very clean and transparent in calm weather. This could mean that fine particles are put in suspension by the waves during windy days, and deposit again on the lake bed during calm days.

3.7 Sources of uncertainty

Besides the specific sources of uncertainty discussed in the sections above, there are other general sources that affect most of the measurements.

3.7.1 Sensor precision and correction for air pressure

The pressure measurements from the sensor are very precise (appendix E). The standard deviation of the water level measurement in the lab is 0.1 mm. However, the measurements on-site might be less precise, primarily because of the correction for air pressure. The measurement of pressure is very sensitive to external factors, such as wind and temperature. As we have no external pressure measurements for comparison, we have to rely on a comparison between our measurements for comparison. The correlation coefficients for the time series of the evaporation pan, Lake 1 and Lake 2 are given in Table 3. Figure 20 shows the time series of air pressure over time.

The slightly lower correlation coefficient for the evaporation pan is due to its construction (2.4): the sensor is fixed inside a metal tube to protect it from vandalism or other potential damages. The pressure inside the tube is slightly higher than the atmospheric pressure outside of it (4.0 mm in average), which results in an overestimation of the atmospheric and subsequently a possible underestimation of the water level in the pan. However, the propagation of this error is unclear, because the water sensor of the evaporation pan is in this tube as well. Very likely, this overpressure also has an influence on the water pressure inside the tube, unless the pressure distribution in the tube is too heterogeneous. As the water height is calculated from the pressure difference, the error most probably cancels in the calculation.

Table 3: Correlation coefficient between the air pressures measured by different sensors.

	Lake 1	**Lake 2**
Evaporation pan	0.889	0.887
Lake 1	-	0.999

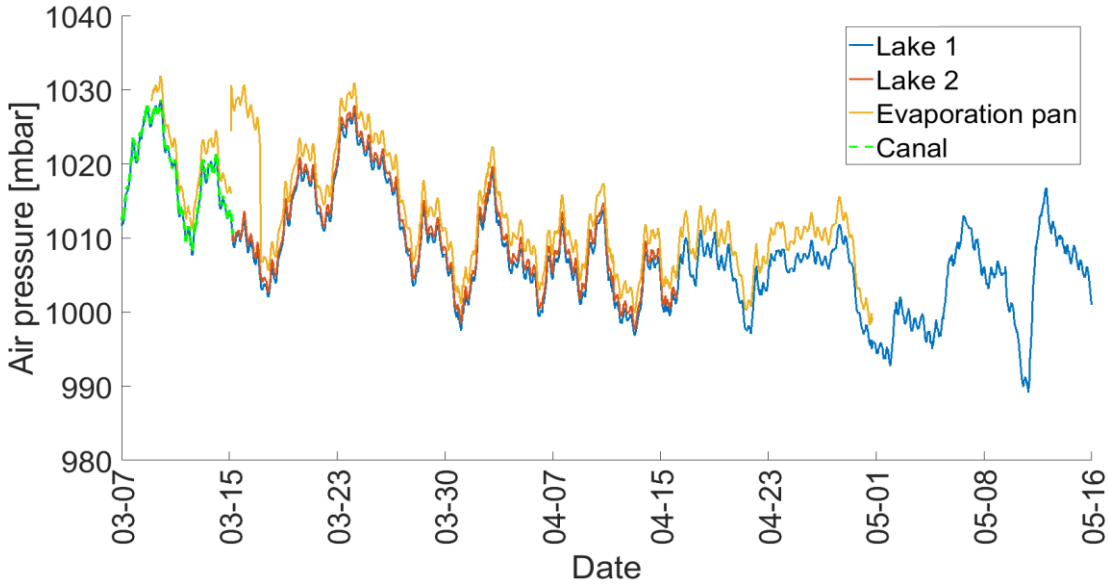

Figure 20: Air pressure at the different location over time. The air pressure at the canal was measured with a double sensor for some days at the beginning of the experiment. Later, a simple sensor was put in Lake 1, and the air pressure was estimated by the mean of the air pressure at lakes 1 and 2.

3.7.2 Precision of the evaporation estimation

The evaporation counts for 11.45% of the water balance during the experiment (3.1.2). An error of 20% in the evaporation estimation, for example, would result in 2.29% of error in the total infiltrated volume, which is low compared to other sources of error.

3.7.3 Influence of wind on the water level

We were not able to find direct measurements of the wind in Guantao. However, the average wind intensity over the study period was between 2 and 3 on the Beaufort scale (between 1.6 m/s to 3.1 m/s and 3.3 m/s to 5.3 m/s) at the weather station of Chaocheng, 60 km south-southeast of Guantao. The wind blew from the north (northeast to northwest) 25% of the time, and from the south (southeast to southwest) 55% of the time.

Lake 1 is a rectangular lake whose length is in the north-south direction. Our sensor is at the southern shore of the lake (2.2, Figure 2). That means that the wind blows over 300 m in one or the other direction. A change in water level between the southern and the norther shore of only 1 cm would be an extremely low gradient, yet it would already influence the measurement of the water level significantly. However, there is no clear quantification of this effect in the literature, so that this remains a supposition.

3.7.4 Hand measurements

The average precision of the hand measurements is ± 3 cm, due to the wave height at the measurement station and the imprecision of the measurement mark. However, the general fit of the hand measurements with the sensor measurement remains very high (3.1.1).

3.7.5 Drone precision

The drone measurements were used to calculate missing geographic data, primarily the slope of the lake shores. Based on that, the average surface of the lake was calculated, and then the total infiltrated volume.

The vertical error of the drone is ± 20 cm according to its producer. The horizontal error is unknown, but as a rough approximation, we shall assume that is it similar to the vertical error. Considering that the lake shores are actually 20 cm smaller than we calculated, we get a difference of 166 m^2. This could lead to an error of 0.4% in the volume estimation, which is very low, given the general imprecision of our data.

3.7.6 Topographic surveying

The dumpy level we could use on-site was very inaccurate: its bias was -1 cm / 10 m length. As a comparison, the tolerated precision for levelling in construction sites in Switzerland is ±0.25 cm / 10 m length.

The measurements were corrected for this inaccuracy. However, the imprecision of the level remains unknown, and is potentially significant. Besides, the measurements were not corrected for usual sources of imprecision, such as light refraction in the atmosphere, due to a lack of time and relevant data.

3.7.7 Interpolation of time series

The measurement time series are an average of the past four minutes. However, the starting point of each time series is different, so that some time series had to be interpolated. The time of measurements were changed, and each quantity was re-calculated as the weighted mean of two quantities. This is of course a source of uncertainty.

3.8 Unknowns

Besides the other unknowns discussed above, the main unknown is the phreatic evaporation and the evapotranspiration. The groundwater table in the area near the lake is close to the ground level, and phreatic evaporation is likely to happen. Likewise, the groundwater level under the lake will remain high for some time after the infiltration is completed. A quantification of the evaporation after infiltration would be useful to quantify the total losses over the infiltration period.

4 Conclusion

The main objective of my thesis was to find the infiltration rate from an artificial lake. This objective has been fulfilled and the infiltration rate during our measurement period is on average 0.037 m/day. The water height has an influence on the infiltration rate, yet the relation it has with the infiltration rate is not straightforward.

The data collected also helped to measure various specifications of the test site. The first is the vertical and horizontal hydraulic conductivities of the clogging layer. They were in the same order of magnitude, with a vertical conductivity of 0.223 m/day and a horizontal conductivity of 0.30 to 0.55 m/day, depending on the assumptions taken. This information will be very useful to model the long-term behaviour of the infiltration lakes. The demonstration of the presence of a clogging layer is in itself an important information for future maintenance and optimisation of the lake.

The total infiltrated volume of approximately 100,000 m^3 per infiltration event is a very useful information for the global water balance model of Guantao.

The hydraulic conductivities at the lake and the canal shores are similar, yet a reliable hypothesis for the infiltration rate for the canal cannot rely solely on this information. Therefore, further research is needed about the infiltration rate from the canal.

5 Outlooks

5.1 Long term behaviour of the lake

Artificial infiltration lakes were built in Guantao as a measure to reach a more sustainable groundwater management. The sustainability of the infiltration lake itself is therefore a central question.

Clogging is very likely to have an effect on the infiltration rate. The reason for this clogging is most probably settlement of fine particles, although this should be investigated further before a conclusion can be drawn. Since the lake is very young, some concerns can be expressed about the effects of clogging on the long-term and the costs of maintenance to avoid it.

Another concern is the reduction of the infiltration rate by a reduction of the Darcy gradient. It was shown that the lake is connected to the aquifer, and therefore the infiltration rate is governed by Darcy's equation. A high table around the lake will form if the infiltration events are too frequent and the volumes too big.

5.2 Artificial infiltration in Guantao on the long term

Artificial infiltration in Guantao was proven useful. Yet on the long-term, some side effects of infiltration may happen. The first one is a rise of groundwater level in the region near the lake. This could put the groundwater in contact with sceptic tanks or other contaminated soils and pollute it. Although this is unlikely in Guantao, as the population density and the industrialisation are low, this should be a general concern in any artificial infiltration project.

5.3 Further investigations and research

The infiltration from the canal remains unknown, yet the hydraulic conductivity is known. A simulation with software solutions such as Geostudio from Geo-Slope or Hydrus from PC-Progess could assess the infiltration rate from the canal. Beside the hydraulic conductivity, the other important data for this model would be the water level in the wells near the canal (if the canal is connected to the aquifer). This can easily be done by a measurement campaign.

A model of the lake with one of the software solutions mentioned above would help to assess the long-term behaviour of the lake and the surrounding groundwater under various scenario. Especially, such a model could predict the general behaviour of the groundwater mound in the lake after an irrigation event. This work could build the basis for a framework for optimal use of the lake and efficient artificial infiltration practices in Guantao. Especially, a calendar of favourable periods for artificial infiltrations could be created. This calendar would take into account the minimal time needed between two infiltration events for the mound to be resorbed, and would find ideal slots during the year, where demand is low (no irrigation) and offer is high (rainy season).

An on-site or simulation study about the lake clogging could create a better understanding of this phenomenon. An analysis of the water quality would be the first step in this study, as it is the primary factor influencing clogging. Subsequently to this study and the model of the lake described above, a conceptual study about alternative layouts for the lake could be conducted. Especially, the use of a sedimentation basin before the infiltration lake would be a solution to investigate. One could also think of solutions making use of the already existing infrastructure,

for example by using one of the two lakes of our test site for sedimentation and the other for the infiltration. Most of the work has already been done, the only infrastructure which is missing is an underground pipe linking the two lakes.

Most of these propositions could be carried out by students as part of their studies. The implication in an international, applied engineering project such as Rehabilitation and Management Strategies for Over-Pumped Aquifers under a Changing Climate would likely be a great personal experience for them like it was for me.

6 Bibliography

ETHZ/IfU and Hydrosolutions ltd (2016). *Annual report (March 2015-March 2016), Handan Region, Rehabilitation and management strategy for over-pumped aquifers under a changing climate*. Zurich.

Bouwer, H. (2002). Artificial recharge of groundwater: Hydrogeology and engineering. *Hydrogeology Journal*, *10*(1), 121–142. http://doi.org/10.1007/s10040-001-0182-4

Chinese Geological Bureau (2015). *Hydrological report of Guantao region*

Konikow, L. F., & Kendy, E. (2005). Groundwater depletion: A global problem. *Hydrogeology Journal*, *13*(1), 317–320. http://doi.org/10.1007/s10040-004-0411-8

Landon, M. ., Rus, D. L., & Harvey, F. E. (2001). Comparison of instream methods for measuring hydraulic conductivity in sandy streambeds. *Ground Water*, *39*(6), 870–885. http://doi.org/10.1111/j.1745-6584.2001.tb02475.x

Linacre, E. T. (1977). A simple formula for estimating evaporation rates in various climates, using temperature data alone. *Agricultural Meteorology*, *18*(6), 409–424. http://doi.org/10.1016/0002-1571(77)90007-3

Molle, F. (2003). *Development Trajectories of River Basins: a Conceptual Framework*.

ETHZ/IfU and Hydrosolutions ltd (2014). *Rehabilitation and management strategy for overpumped aquifers under a changing climate in China: Project proposal*.

Taylor, R. G. (2012). Ground water and climate change. *Nature Climate Change*, *3*(April), 322–329. http://doi.org/10.1038/NCLIMATE1744

Appendices

A. Aerial picture from drone flight

B. Timeline of the experiment

Date		China	Switzerland
February	08-14		
	15-21		Preparation of the experiment in Swziterland
	22-28		
March	29-06		
	07-13	Setup of the experiment in Guantao. Schooling of the students	
	14-20		
	21-27		
	28-03	29.03: Data reading 03.04: Data reading	Data analysis in Switzerland
April	04-10		
	11-17	16.03: Data reading	
	18-24		
	25-01	30.04: Data reading	
May	02-08		
	09-15	approx. 10.05: lake 1 dried out dismantling of the experiment on-site	
	16-22	16.05: Data reading	
	23-29		
June	30-05		
	06-12		Final presentation
	13-19		
	20-26	Prof. Kinzelbach takes the experiment material back to Zurich	Final report
	27-03		

C. Data collection sheet

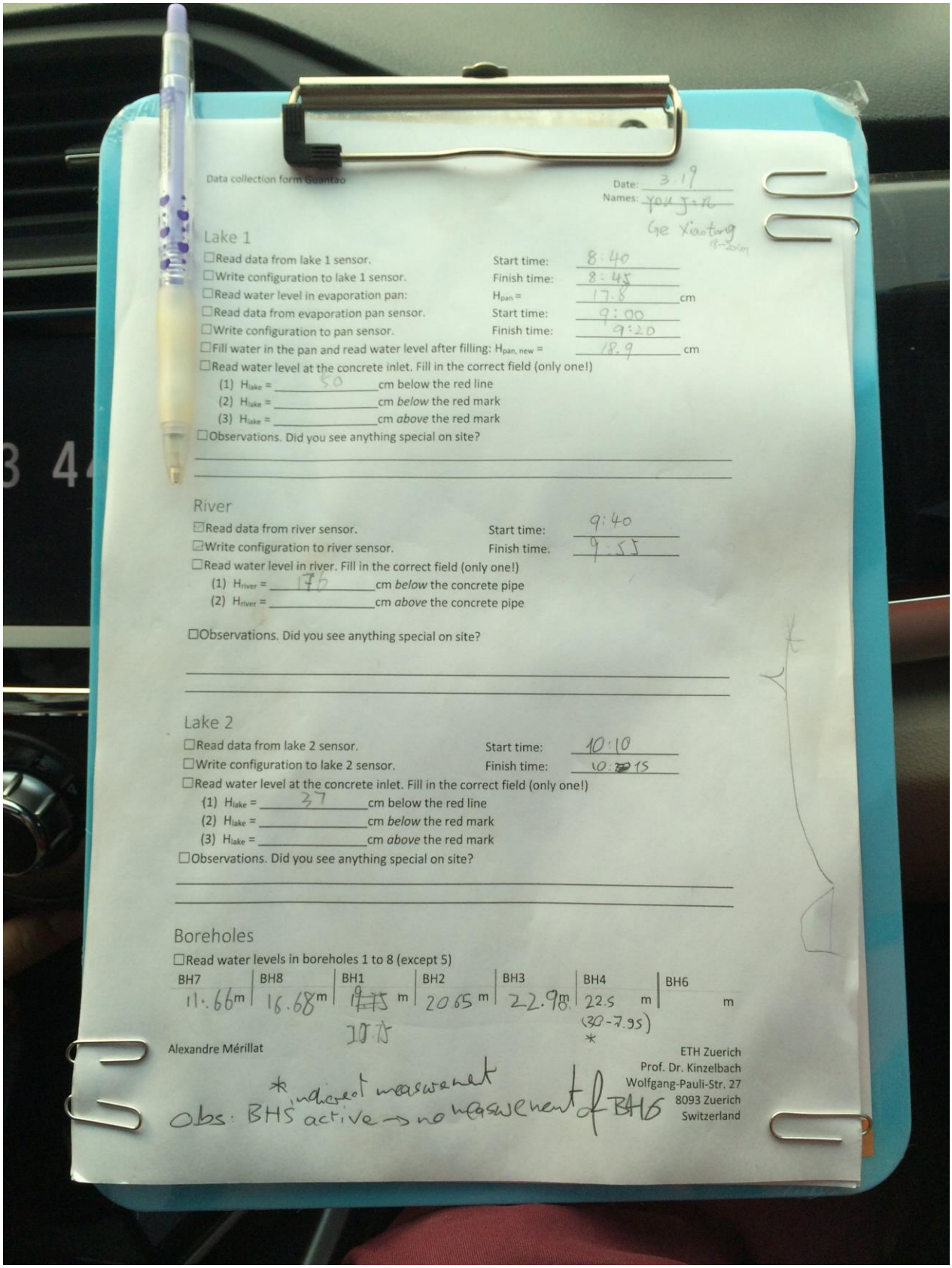

Data collection form Guantao

Date: 3.19

Names: ~~You Jia~~ Ge Xiaotong 18-Zürich

Lake 1

☐Read data from lake 1 sensor. Start time: 8:40

☐Write configuration to lake 1 sensor. Finish time: 8:45

☐Read water level in evaporation pan: H_{pan} = 17.8 cm

☐Read data from evaporation pan sensor. Start time: 9:00

☐Write configuration to pan sensor. Finish time: 9:20

☐Fill water in the pan and read water level after filling: $H_{pan,\ new}$ = 18.9 cm

☐Read water level at the concrete inlet. Fill in the correct field (only one!)

(1) H_{lake} = 50 cm below the red line

(2) H_{lake} = _____ cm *below* the red mark

(3) H_{lake} = _____ cm *above* the red mark

☐Observations. Did you see anything special on site?

River

☐Read data from river sensor. Start time: 9:40

☐Write configuration to river sensor. Finish time: 9:55

☐Read water level in river. Fill in the correct field (only one!)

(1) H_{river} = 176 cm *below* the concrete pipe

(2) H_{river} = _____ cm *above* the concrete pipe

☐Observations. Did you see anything special on site?

Lake 2

☐Read data from lake 2 sensor. Start time: 10:10

☐Write configuration to lake 2 sensor. Finish time: 10:15

☐Read water level at the concrete inlet. Fill in the correct field (only one!)

(1) H_{lake} = 37 cm below the red line

(2) H_{lake} = _____ cm *below* the red mark

(3) H_{lake} = _____ cm *above* the red mark

☐Observations. Did you see anything special on site?

Boreholes

☐Read water levels in boreholes 1 to 8 (except 5)

BH7	BH8	BH1	BH2	BH3	BH4	BH6
11.66 m	16.68 m	~~19.75~~ 18.15 m	20.65 m	22.9 m	22.5 m (30-7.95) *	m

Alexandre Mérillat

ETH Zuerich
Prof. Dr. Kinzelbach
Wolfgang-Pauli-Str. 27
8093 Zuerich
Switzerland

* indirect measurement

obs: BH5 active → no measurement of BH6

D. Creation of the water level time series

The water level were recorded based on the pressure time series of the sensors and hand measurements. The raw data from the logger bring little information about the true water height, because the sensors have been moved multiple times and the elevation of the sensor is not known a priori. Therefore, the data must be corrected.

Most change of sensor position were recorded in a separate file. The others were detected visually, as they produce a perturbation (sudden surge or fall) in the pressure time series. For each perturbation, the slope of the time series before the event was calculated by taking the average slope between the last point before the perturbation and a point three days before the current perturbation. If the previous perturbation happened less than three days before, the first point was used to calculate the slope. The corrected position of the curve after the perturbation was calculated from this slope and the duration of the perturbation. A loop was created to correct the changes of position one after the other, starting with the first. The resulting time series shows the correct changes of water level over time, but it is not expressed in a reference frame linked to the surrounding environment. The link between this time series and the surrounding environment is done by fitting the time series to the hand measurements with the least-squares method. After that, the water table elevation can be compared to other quantities, such as the depth of the lake or the water table in the wells.

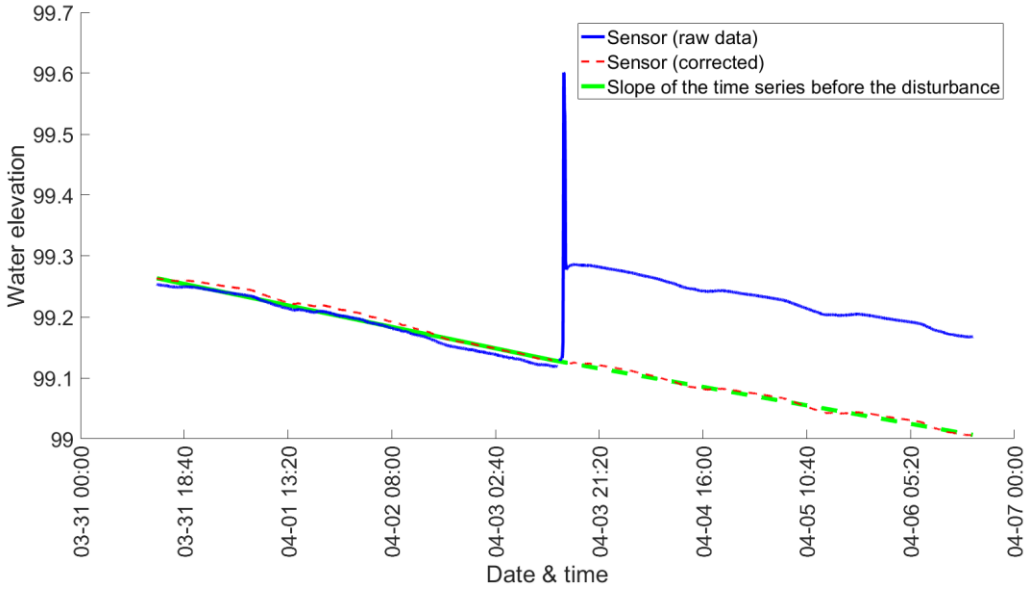

Figure 21: correction process of sensor data.

E. Sensor precision

The sensor precision was tested in the ETH laboratory. Two sensors were placed in two different beakers filled with water and measured the water and air pressures. One logger recorded the measurement every second, while the other recorded the average over one minute. Both setups were placed in a closed fume hood with the ventilation switched off to avoid any influence from air movement.

Both series were corrected for the linear trend due to evaporation loss. The standard deviation of the corrected 1-min-average series is 0.10 mm, while the standard deviation of the 1-sec-interval series is 0.39 mm. Figure 22 shows the time series from the two sensors.

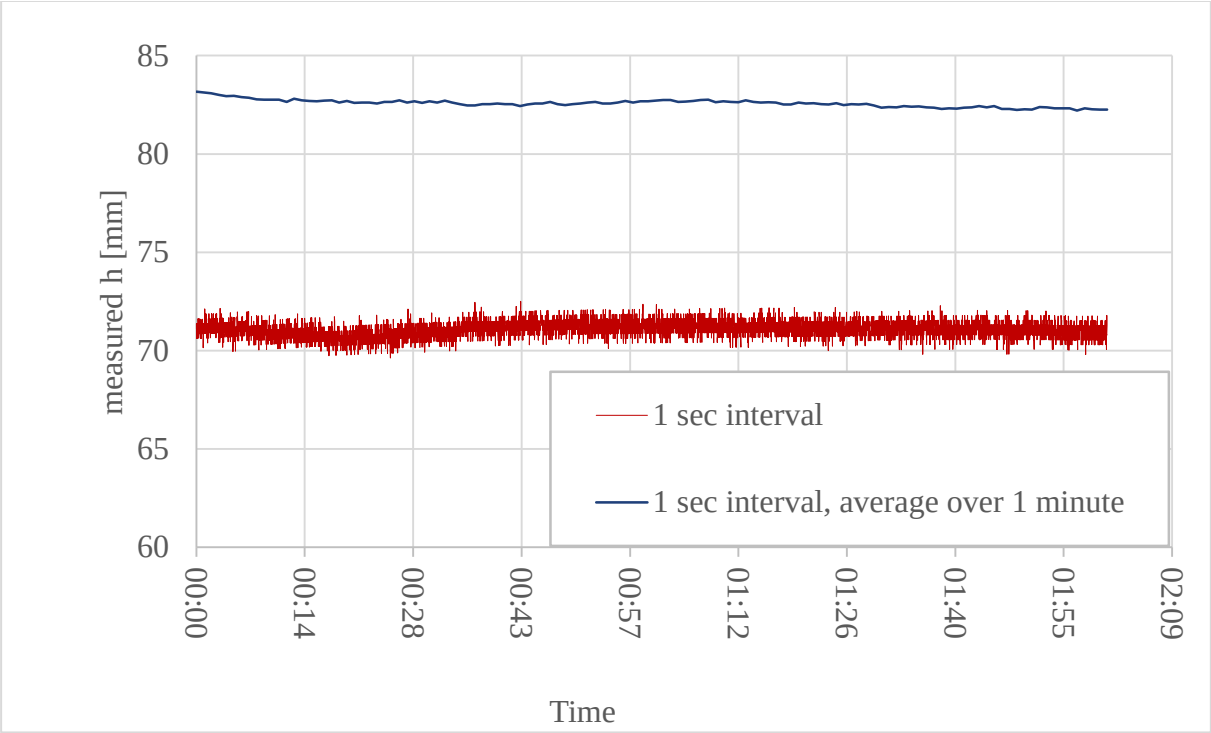

Figure 22: time series of water pressure measurements with two different logger configurations. One series was recorded with an interval of one second, the other with an average over one minute.

Contact

ETH Zurich
Institute of Environmental Engineering
Wolfgang-Pauli-Str. 15
8093 Zurich
Switzerland
www.ifu.ethz.ch